Unraveling the molecular basis of antibiotic resistance in *Staphylococcus aureus,* focusing on plasmid-mediated mechanisms

Kiran Fatima[1]*, Kashif Ali[1], Khwaja Ali Hasan[2], Neha Farid[1], Asma Bashir[1], Mumtaz Hussain[3], Shahab Mehmood[1] and Zahid Hussain[3]

[1]Department of Biosciences, Faculty of Life Sciences, Shaheed Zulfikar Ali Bhutto Institute of Science and Technology (SZABIST) University, Karachi, Pakistan
[2]Molecular Biology & Structural Biochemistry Research Laboratory, Department of Biochemistry, University of Karachi, Karachi, Pakistan
[3]Department of Chemistry, University of Karachi, Karachi, Pakistan

Abstract: This study investigates antibiotic resistance mechanisms in *Staphylococcus aureus*, focusing on plasmid-mediated resistance, and evaluates triazole compounds as potential inhibitors against resistant strains. The study was conducted at SZABIST, Karachi, using ten *Staphylococcus* isolates. Identification was performed via biochemical assays and 16S rRNA PCR. Antibiotic resistance was assessed and the RepA gene, responsible for plasmid-mediated resistance, was detected. In-silico molecular docking studies were conducted with triazole compounds (C1, C2, C3, C4). Statistical analysis was performed using SPSS, and ANOVA was used to assess significant differences. *S. aureus* exhibited resistance to methicillin and vancomycin. 75% of isolates did not produce biofilm. PCR revealed the presence of the RepA gene. Among the compounds tested, C3 showed the strongest antimicrobial activity and stable binding interactions with RepA. The study concluded that resistance in clinical *S. aureus* strains is not encoded by mecA and vanA genes but rather by the plasmid-mediated RepA gene. Compound C3 emerged as a potent inhibitor, offering a promising direction for future research in combating multidrug-resistant *S. aureus* strains.

Keywords: Vancomycin resistance *Staphylococcus aureus* (VRSA), methicillin resistance *Staphylococcus aureus* (MRSA), molecular mechanism, antimicrobial resistance

INTRODUCTION

Antimicrobial Resistance (AMR) continues to be a growing global issue, primarily caused by the widespread and often inappropriate use of antibiotics. It is estimated that 70% of antimicrobial use is linked to human medicine and agriculture, contributing significantly to AMR (World Health Organization (WHO, 2021). AMR remains a dynamic risk to public health worldwide, exacerbating mortality and morbidity rates. The World Health Organization (WHO) has projected that 10 million deaths per year could result from AMR by 2050 if current trends continue (WHO, 2019). Infections caused by antibiotic-resistant bacteria lead to twice as many adverse clinical outcomes and substantially higher healthcare costs compared to infections caused by susceptible strains (Friedman *et al*., 2016; Jalal *et al*., 2021). Methicillin-resistant *Staphylococcus aureus* (MRSA) is a significant contributor to Healthcare-Associated Infections (HAIs), becoming increasingly difficult to treat due to its growing resistance to available antibiotics (Enright *et al*., 2002). Resistance to antibiotics is a widespread issue, especially with *S. aureus*. Multiple studies have reported the isolation of single- or multidrug-resistant *S. aureus* strains from numerous sources, including healthcare facilities, food and the environment (Deschaght *et al*., 2009; Kallen

et al., 2010). The mecA gene, which confers resistance to methicillin, is carried by the Staphylococcal cassette chromosome mec (SCCmec) (Omrani-Navai *et al*., 2017). Identifying the mecA and VanA genes is critical for understanding resistance in *S. aureus* (Becker *et al*., 2018). A plasmid that harbors multidrug-resistant genes can encode additional resistance mechanisms against various antibiotics. The RepA resistance gene, which is located on the plasmid, contributes to antibiotic resistance and the metabolism of foreign substances, such as hydrocarbons and lactose, through catabolic pathways (Schumacher *et al*., 2014). Plasmid curing is a method to counteract antimicrobial resistance, and it involves the use of chemical and physical methods to remove the plasmid from bacteria. For *S. aureus*, chemical agents such as Acridine Orange Base (AOB) and Ethidium Bromide (EtBr) have been employed for plasmid curing. The RepA gene plays an essential role in regulating virulence and resistance mechanisms in *S. aureus* (Schumacher *et al*., 2014). The RepA protein, a plasmid-encoded replication initiator, is crucial for the transmission and propagation of resistance determinants. Consequently, understanding how RepA mediates resistance in *S. aureus* is vital for developing new therapeutic strategies (Schumacher *et al*., 2014). Methicillin-resistant *S. aureus* (MRSA) is particularly concerning due to its ability to spread its resistance traits to other harmful strains through food supplies, genetic material in bacteria, and plasmids

*Corresponding author: e-mail: kiranfatima14@gmail.com

(Biswas *et al*., 2015). This highlights the urgent need for alternative therapies to combat infections without exacerbating resistance to new drugs. In this context, novel triazole compounds have been synthesized and screened for their antibacterial efficacy against MRSA and vancomycin-resistant *S. aureus* (VRSA) isolates. Structural characterization of the interactions between these compounds and their target proteins is crucial for the rational design of therapies with reduced toxicity and improved antibacterial activity (Rashdan and Shehadi, 2022). The objective of the present research was to investigate the resistance mechanisms of MRSA and VRSA isolates from various sources and assess the potential inhibitory effects of synthesized chemicals against the RepA-resistant protein. The study also aimed to provide valuable insights into the prevalence and characteristics of *S. aureus* from diverse samples, including clinical strains, soil, water and yogurt.

MATERIALS AND METHODS

Characterization, Analytical Techniques and Compound Synthesis
Analytical grade reagents and solvents were purified using Silica gel 60 Fluka and Thin Layer Chromatography (TLC). The structural characterization of compounds was conducted using1 H-NMR (Bruker Avance 300 MHz), EI-MS (JEOLJMS-600), FT-IR (VECTOR 22, BRUKER), and elemental analysis. Triazole compounds ($4C_1$-C_4) were synthesized following Zhang *et al*. (Zhang *et al*., 2005), Alkyl azides ($3C_1$-C_4) were produced by refluxing compounds ($2C_1$-C_4) with sodium azide. The alkyne molecule (1C) was prepared by reacting propargyl bromide with vanillin using potassium carbonate. Azides ($3C_1$-C_4) were then reacted with (1C) in the presence of a Cu(I) catalyst, prepared by reducing CuSO4.5H2O with sodium ascorbate, producing($4C_1$-C_4) with good efficiency. The structural properties of the synthesized triazoles were verified using IR, NMR, mass spectrometry, and elemental analysis.

Isolation and Characterization of Staphylococcus aureus
Ten staphylococcal strains were isolated from tap water, garden soil, food, and clinical samples, cultured on Mannitol Salt Agar (MSA), and incubated at 37°C for 24 hours (Zhang *et al*., 2005). *Staphylococcus aureus* colonies were purified using the four-streak method, and incubated at 37°C for 24 hours. Identification was performed using Gram staining, morphological characterization, and biochemical tests, including the catalase test, coagulase test, salt tolerance, mannitol fermentation, and hemolytic activity on 5% sheep blood agar (Rodgers *et al*., 1999; Morris *et al*., 2001). Biofilm formation was also included as part of the phenotypic characterization, to understand the pathogenic potential of the isolates.

Molecular Identification of 16S rRNA Gene
The genomic DNA of *Staphylococcus aureus* was isolated using the EZ-10 Spin Column Bacterial Genomic DNA Miniprep Kit and its purity and concentration were assessed using a NanoDrop spectrophotometer (Zoetendal *et al*., 2006). The highly conserved regions at the species level were confirmed using 16S rRNA multiplex PCR using set primers 27F and 1492R. The Multiplex PCR protocol involves an initialization of denaturation with 35 cycles at 94ºC, for 2 minutes, annealing at 50ºC for 30 seconds, and elongation at 72ºC for 45 seconds. The final extension step occurs at 72ºC for 4 minutes. A positive control, *S. aureus* ATCC 25923, was used. PCR product purification was performed using a Biobase purification kit and quantification was done using a NanoDrop spectrophotometer. Sequencing for the required PCR product was performed by Macrogen. The experiment aimed to identify highly conserved regions at the species level (Thwala *et al*., 2022).

Detection of Resistance-Encoding Genes
PCR amplification was performed to assess resistance-encoding genes in *Staphylococcus aureus*. Specific primers were used for *mecA* F (3'- AGAAGATGGTATG TGGAAGTTAG -5') and R (5'- ATGTATGTGCGATTG TATTGC -3'), and vanA F (3'- GGCAAGTCAGGTGAA GATG -5') and R (5'- ATCAAGCGGTCAATCAGTTC -3'), were used to amplify the targets. Housekeeping gene aroE (5'-ATCGGAAATCCTATTTCACATTC-3') R (5'-GGTGTTGTATTAATAACGATATC-3') and *Staphylococcus aureus* ATCC 29213 were used as a positive control for amplification as it had the two resistant genes of *mecA* and *vanA*. Amplification was conducted using a thermal cycler (Eppendorf, Germany) under conditions of initial denaturation at 95°C for 2 minutes, followed by 35 cycles of 94°C for 1 minute, annealing at 50°C for 50 seconds, and elongation at 52°C for 40 seconds (Tamura *et al*., 2011). PCR products were analyzed with a 100bp DNA ladder on a 1% agarose gel to confirm size and purity.

Detection of Biofilm Formation by MtP and CRA
Biofilm formation by *S. aureus* strains was performed using the Microtiter Plate (MtP) assay and Congo Red Agar (CRA) assay. For the MtP assay, *S. aureus* strains were incubated for 24 hours at 37°C on blood agar (BD Diagnostics). The strains were diluted 1:200 in trypticase soy broth (TSB; Sigma-Aldrich), supplemented with 0.25% glucose, and transferred to a 96-well microtiter plate. The plate was then incubated at 37°C for 18 h, followed by washing with phosphate-buffered saline (pH 7.2). The remaining biofilm was stained with crystal violet (ELI Tech Group Biomedical Systems), incubated for 1 min at room temperature, and let dry, then solubilized in 1% w/v SDS. Optical density at 490 nm (O.D490) was read on a spectrophotometer (Thermo Fisher Scientific). TSB was used as a blank, with *S.*

aureus ATCC 35984 as the positive control and *S. aureus* ATCC 12228 as the negative control, as described by Sofy *et al*. (2020) and Treves (2010). For the CRA Assay. The formation of biofilm was assayed by growing *S. aureus* on Congo Red Agar (CRA) at 37°C for 24 h as described by Freeman *et al*. (1989). The CRA-positive isolates formed black colonies, whereas the CRA-negative isolates appeared red.

Assessment of the antimicrobial efficacy and determination of the minimum inhibitory concentration (MIC)

The *Staphylococcus aureus* strains were identified as MRSA and VRSA using the disk diffusion method. Antibiotic susceptibility was tested using discs of Sparfloxacin (30µg), Ciprofloxacin (5µg), Cephalexin (30µg), Clindamycin (2µg), Linezolid (30µg), Amikacin (30µg), Methicillin (5µg), Vancomycin (30µg), Compound Sulphamide (300µg), Streptomycin (10µg), Levofloxacin (30µg), Oxacillin (5µg) and Daptomycin (30µg). Testing followed standard reference guidelines (Patel *et al*., 2015), with bacterial suspensions adjusted to the 0.5 McFarland Turbidity standard. Zones of inhibition were measured after 24 hours of incubation at 37°C. Minimum inhibitory concentrations (MICs) for ineffective antibiotics were determined using the E-test method (Georgieva *et al*., 2008).

Plasmid curing and intercalating agents

Bacterial suspensions grown in Luria Bertani Broth (LB) were prepared as 0.5 McFarland Turbidity standard. In tubes containing 5ml of bacterial culture, 50µl of Acridine orange and Ethidium Bromide, each of 0.5mg/ml, were added separately and incubated at 37°C for 24 hours (Liu *et al*., 2012). After incubation, an antibiogram assay was done as performed earlier (Leshem *et al*., 2022).

In silico analysis
Protein retrieval and preparation

The 3D protein structure essential for molecular docking was downloaded from the PDB database or modeled using SWISSMODEL in cases where no structure was available (Kiefer *et al*., 2009). Protein preparation included removing extraneous molecules using UCSF Chimera, adding hydrogen atoms, and incorporating Kollman charges through AutoDock v4.2 (Huey *et al*., 2012; Morris *et al*., 2001).

Compound retrieval and preparation

Synthesized triazole-based compounds (C1–C4) were converted to 3D PDB files using Open Babel (O'Boyle *et al*., 2011) (table 1). Their energy minimization was performed using the FROG2 program with MMFF94 force fields over 1500 steps (Miteva *et al*., 2010; Jalal *et al*., 2021). The prepared compounds were saved in PDBQT format for molecular docking.

Molecular docking studies

The assessment of binding affinities and inhibitory activities of the compounds was conducted through the application of the Lamarckian Genetic Algorithm utilizing AutoDock v4.2. A grid box was positioned at the receptor's active site, characterized by grid center parameters of -8.444, -9.833, and -3.278, alongside dimensions measuring 66 × 60 × 62 points along the X, Y, and Z axes, respectively. The algorithm executed a total of 250 runs, with the maximum generation threshold established at 27,000 and the maximum evaluation limit set at 250,000 (Jalal *et al*., 2021).

ADME profiling and toxicity analysis

Physicochemical properties, bioavailability, and drug-likeness were evaluated using SwissADME (Georgieva *et al*., 2008). ADME profiling included assessments of absorption, distribution, metabolism, and excretion. Toxicity was analyzed using the pkcsm program, which predicted acute toxicity in rats and mice, carcinogenicity patterns and overall safety profiles.

STATISTICAL ANALYSIS

The SPSS (v. 25) was used to analyze the data. The quantitative variables were subjected to a Mean and Standard Deviation analysis. We used Analysis of Variance (ANOVA) to compare the zone sizes. The statistical significance level used was $p \leq 0.05$.

RESULTS

Identification of 16S rRNA

Amplification of the desired DNA sequence of *S. aureus* genes was detected using primers of 16S rRNA after PCR amplification of genomic DNA with 100-500bp. The end product of PCR was evaluated through 1% agarose gel electrophoresis and PCR amplicon was determined with reference to 1 kbp DNA ladder (fig. 1A).

Phylogenetic clustering of S. aureus

The sequencing of 16S rRNA was done at Macrogen, located in Korea, using purified amplicons. The 16S ribosomal RNA (rRNA) sequences were obtained from the National Center for Biotechnology Information (NCBI) database, and the Basic Local Alignment Search Tool (BLAST) was used to compare the adjacent sequences. Nucleotide sequences were used to generate a phylogenetic tree in the program Molecular Evolutionary Genetic Analysis (MEGA-6) (Turnipseed, 2022). Consequently, it was observed that these identified strains belonged to the MRSA-resistant family thus confirming the characterization process (fig. 1B).

Table 1: Synthesized triazole composites details utilized in the current study as 1, 2, 3, and 4 with IUPAC names and structures.

S. No	Compound ID	Compound Name	Compound Structure
1	C1	4-(2-(5-((4-bromophenoxy) methyl)-1H-1,2,3-triazol-1-yl) ethoxy)-3-methoxybenzaldehyde	
2	C2	3-methoxy-4-(2-(5-((naphthalen-1-yloxy) methyl)-1H-1,2,3-triazol-1-yl) ethoxy) benzaldehyde	
3	C3	3-methoxy-4-(2-(5-((naphthalen-2-yloxy) methyl)-1H-1,2,3-triazol-1-yl) ethoxy) benzaldehyde	
4	C4	4,4'-(((5,5'-((1,3-phenylenebis(oxy))bis(methylene))bis(1H-1,2,3-triazole-5,1-diyl))bis(ethane-2,1-diyl))bis(oxy))bis(3-methoxybenzaldehyde)	

**Table 2**: The 16S rRNA, *mecA, vanA, and aroE* primer sequences of *S. aureus*

| Primer		Direction of Sequences	Amplicon sizes (bp)
16S rRNA	27F (3'_5')	AGAGTTTGATCCTGGCTCAG	500bp
	1492R (5'_3')	TACGGTTACCTTGTTACGACTT	
mecA	F	GTAGAAATGACTGAACGTCCGATGA	310bp
	R	CCAATTCCACATTGTTTCGGTCTAA	
vanA	F	GGCAAGTCAGGTGAAGATG	713 bp
	R	ATCAAGCGGTCAATCAGTTC	
aroE	F	ATCGGAAATCCTATTTCACATTC	450 bp
	R	GGTGTTGTATTAATAACGATATC	
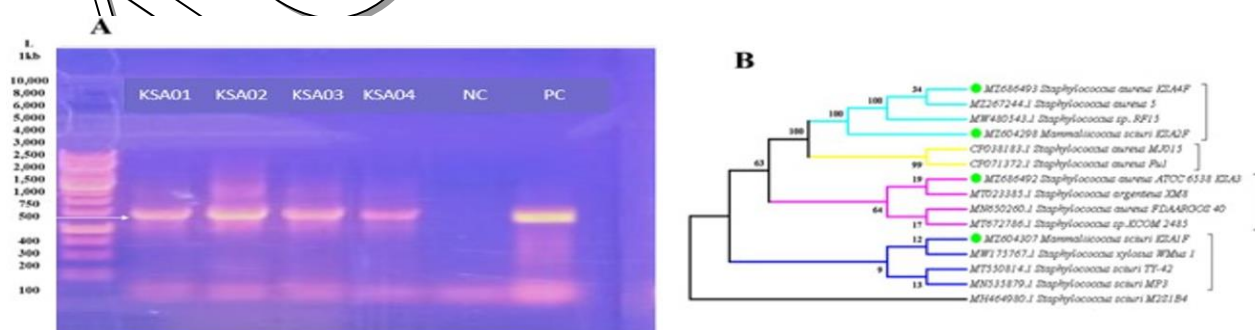
Fig. 1: (A) shows the 16 rRNA amplicon PCR findings for the strains of *S. aureus*. Lane 1: DNA marker (1kb); Lanes 2 to 5 shows the strains of KSA01, KSA02, KSA03 and KSA04; Lanes 6 shows Negative Control (NC) and Lanes 7 shows Positive Control (PC) (ATCC 33591); (B) Phylogenetic Tree created using 16s rDNA sequence amplified from genomic DNA of MRSA and other strains derived from BLAST findings to confirm the reliability and assess the similarity between *Staphylococcus aureus* strains.

Table 3: The tables represent the weak/no biofilm formed according to Ref. value as Weak<0.120, Moderate 0.120-0.199, High0.200-0.239, Strong high >0.240, Wavelength (OD490)

S. No.	Strain	Mean OD value	Biofilm formation	Ref. value	
1	KSA 01	0.01	None/ Weak	<0.120	None/Weak
2	KSA 02	0.003	None/ Weak	0.120-0.199	Weak
3	KSA 03	0.00	None/ Weak	0.200-0.239	Moderate
4	KSA 04	0.00	None/ Weak	>0.240	High/Strong
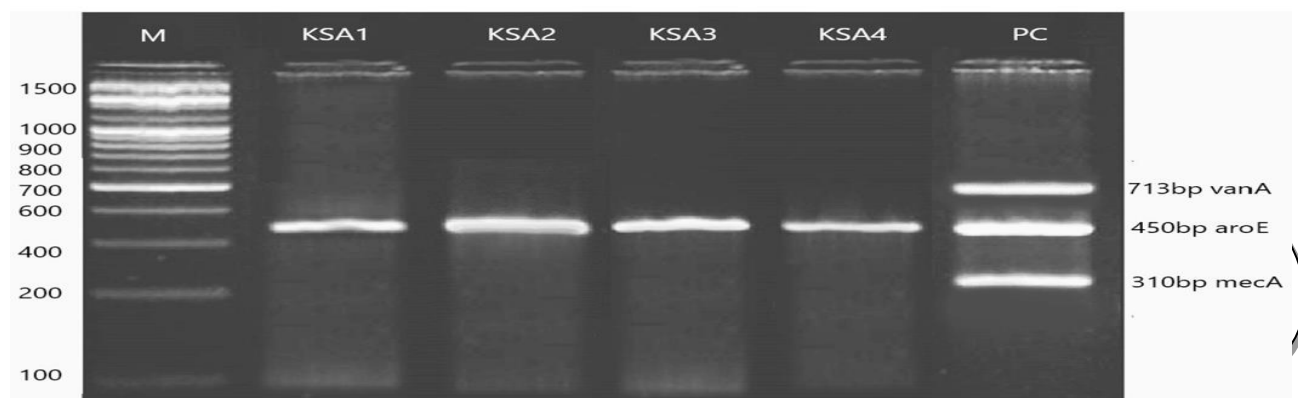
Fig. 2: The PCR results of the *mecA, vanA* gene for *S. aureus* strains. Lane 1: DNA marker (100bp); Lanes 2, 3, 4 & 5 *S. aureus* samples; Lane 6: Positive control (ATCC 33591). No resistant Genes were found except housekeeping (*aroE*) gene.
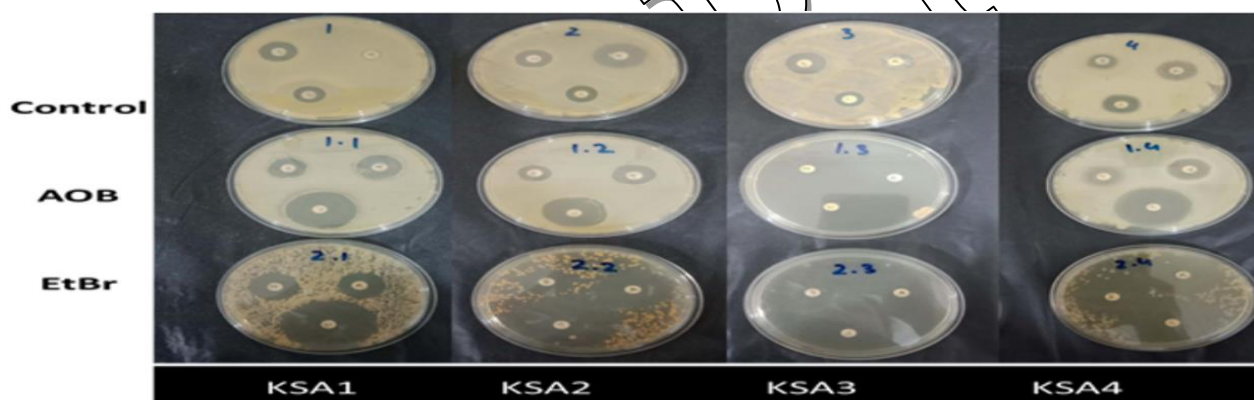

Fig. 3: Control with plasmid and AOB & EtBr without plasmid. Control strains show resistivity, while treated with curing agents show sensitivity against *S. aureus*.

Table 4: ADME properties analysis of shortlisted compounds

Name	Water Solubility	CaCo2 permeability	HIA	Skin Permeability	BBB permeability	Lipinski Violation	Bioavailability radar
C1	-4.537	0.994	94.403	-2.736	No	Yes	
C2	-4.823	0.931	94.023	-3.228	Yes	Yes	
C3	-4.849	0.902	93.996	-3.226	Yes	Yes	
C4	-4.329	0.153	78.912	-2.664	No	No	

Pak. J. Pharm. Sci., Vol.38, No.2, March-April 2025, pp.001-011

5
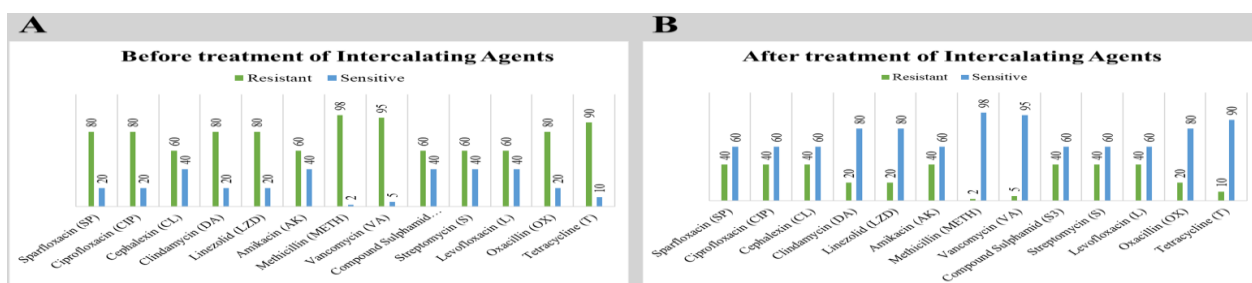
Fig. 4: (A) Result of antibiotics susceptibility test on *S. aureus* isolates before plasmid treatment with intercalating agent (B) Result of antibiotics susceptibility rate on *S. aureus* isolates after plasmid treatment with intercalating agent.
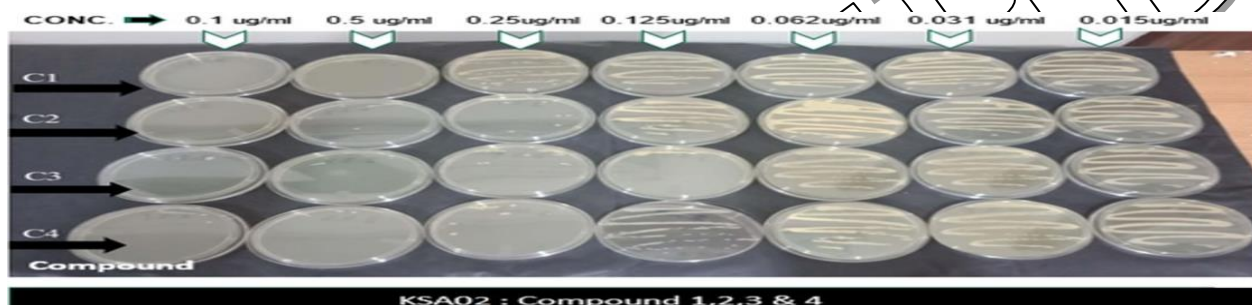

Fig. 5: Antimicrobial activity of synthesized compounds showing the inhibition of *S. aureus* in different concentrations. The compound C3 shows the most potential activity for *S. aureus* inhibition.

**Table 5**: Toxicity analysis of four shortlisted compounds

Name	Max. tolerated dose (human)	Min. now toxicity	*T. Pyriformis* toxicity	Oral Rat Acute Toxicity (LD50)	Ames Test	Hepatotoxic	Skin Sensitization
C1	-0.271	1.566	0.591	2.943	Yes	Yes	No
C2	-0.84	0.241	0.557	3.255	No	No	No
C3	-0.853	0.199	0.561	3.244	No	No	No
C4	-0.497	2.031	0.285	3.168	No	Yes	No

Table 6: The interaction detail of shortlisted compound

Compound	Ligand	Receptor	Interaction	Distance	E (kcal/mol)	Binding score (kcal/mol)	Predicted Ki (µm)
C1	O7	CB LYS 85	H-acceptor	2.83	-0.5		
	N12	NZ LYS 88	H-acceptor	3.03	-3.7		
	N13	NZ LYS 88	H-acceptor	2.83	-6.0	-5.11	180.84
	N14	CA LYS 85	H-acceptor	3.28	-0.7		
	O27	CA GLU 89	H-acceptor	2.82	-0.7		
C2	N12	O TYR 18	H-donor	2.93	-0.9		
	N12	CA GLN 19	H-acceptor	3.06	-1.5		
	N12	N LEU 20	H-acceptor	2.75	-5.0	-6.94	8.23
	N13	N LEU 20	H-acceptor	3.08	-0.7		
	N13	CB LEU 20	H-acceptor	3.29	-0.8		
C3	N16	O TYR 18	H-donor	2.63	-0.8		
	N15	CA GLN 19	H-acceptor	3.32	-0.9		
	N17	CB LEU 20	H-acceptor	3.49	-0.7	-7.34	4.15
	O30	CA PHE 17	H-acceptor	3.41	-0.7		
	O30	N TYR 18	H-acceptor	3.03	-2.5		
C4	N12	O ARG 16	H-donor	2.55	-1.1		
	N33	N LEU 20	H-acceptor	3.08	-4.4		
	O36	CA GLN 19	H-acceptor	3.67	-0.5	-5.48	96.18
	O43	NE2 GLN 19	H-acceptor	3.22	-1.0		
	O26	N ARG 16	H-acceptor	3.44	-0.7		
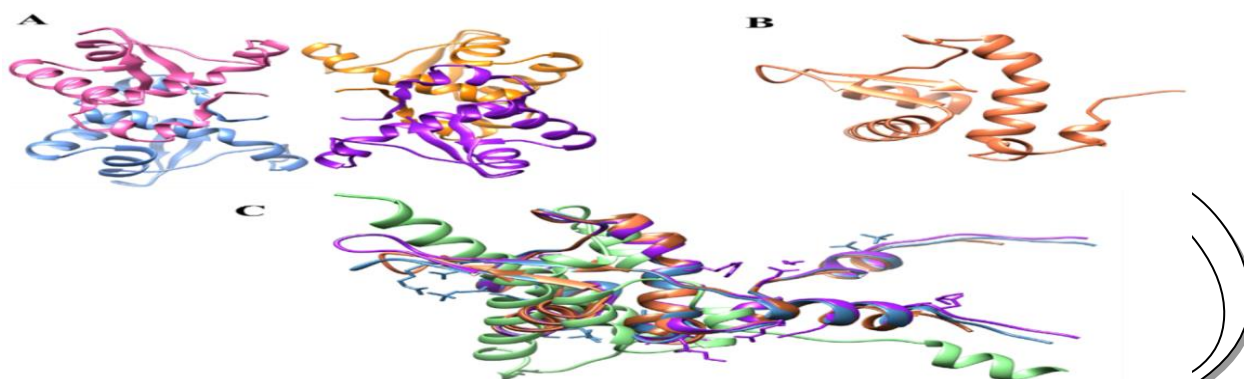
Fig. 6: The 3D structure of RepA modeled via SWISSMODEL (A) tetramer (B) Monomer (chain A), and (C) model protein (coral) superimposed on the templates 4PQK (green), 4PTA (sienna), 4PQL (purple), and 4PT7 (steel blue).
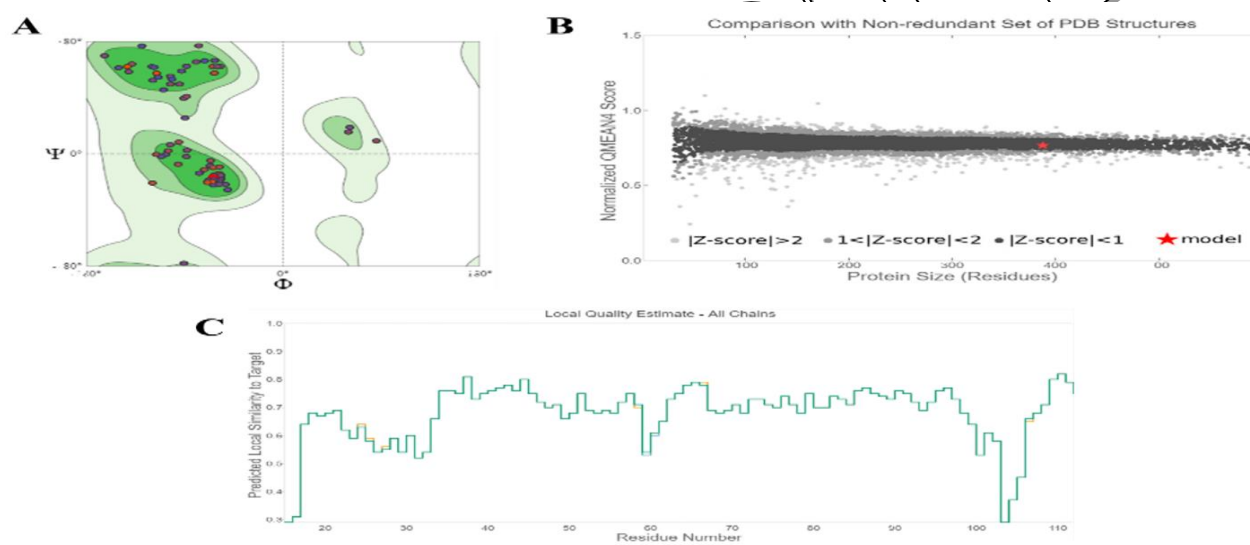
Fig. 7: Validation of RepA modeled structure through SWISSMODEL. (A) Ramachandran Plot showing the 96% residues of protein within the allowed region, (B) z-score generated showing the validity of modeled structure i.e., <1, and (C) quality prediction of protein structure.
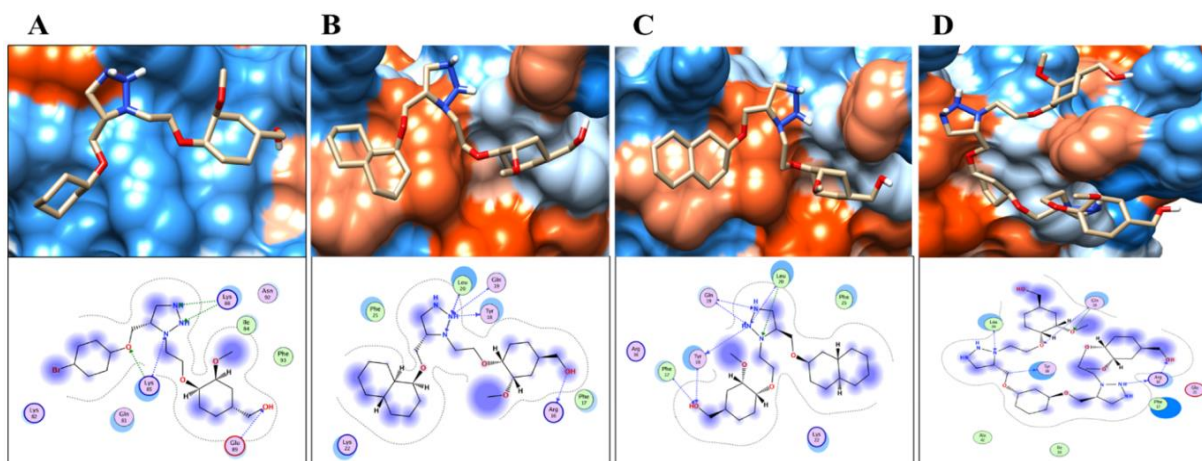
Fig. 8: Docking studies of (A) C1, (B) C2, (C) C3 and (D) C4 generated through MOE tool.

Pak. J. Pharm. Sci., Vol.38, No.2, March-April 2025, pp.001-011

7

PCR screening for resistance & housekeeping genes

The resistance *mec*A and *van*A genes were not found in the isolates of *Staphylococcus aureus* by using PCR with a specific primer. The results obtained are highlighted in the fig. 2.

Biofilms analysis

Detection of biofilm formation using the micro titer-plate (MtP) assay

According to the MtP assay, *S. aureus* strains exhibiting an O.D.490 reference value below 0.1 were classified as non-producers, while those with an O.D.490 value ranging from 0.1 to 1.0 were considered weak biofilm producers. On the other hand, strains with an O.D.490 value above 1.0 were identified as strong biofilm producers (table 4). Duplicate strains of each species were used in three separate biofilm formation assays (Treves, 2010).

Detection of biofilm formation by CRA assay

The characterization of the isolates was based on the morphological appearance of the colony. Strong biofilm producers were observed to form black colonies, while moderate biofilm producers formed blackish-red colonies. Weak or non-producers were observed to form pink colonies. Each strain was tested according to triplicate testing for biofilm production (Schumacher *et al*., 2014).

Plasmid curing in bacteria with intercalating agents

Curing the bacterial plasmid was done with the intercalating agents: Acridine Orange Base (AOB) and Ethidium Bromide (EtBr) at a 0.5 mg/mL concentration. As seen in fig. 3, the control strains with plasmids that expressed resistance to the antibiotics showed a smaller zone of inhibition, whereas the strains treated with AOB & EtBr were found to be sensitive to the antibiotics. This is due to the removal of plasmids by treating them with curing agents. It led to the fact that the antibiotic resistance in the strains was contributed by the plasmid. It was also observed that EtBr has more potential as a plasmid curing agent as compared to AOB.

Difference in antibiotic susceptibility pattern before and after treatment of curing agent

Before treatment with the curing agent, *Staphylococcus aureus* strains showed high resistance to multiple antibiotics, with MRSA prevalence higher than 90% and resistance rates between 80% and 100%. The major resistance rates were as follows: Methicillin (100%), Vancomycin (95%), Daptomycin (95%), and Sparfloxacin (80%) (fig. 4a) (Becker *et al*., 2018; Jalal *et al*., 2021).

After treatment with intercalating agents, a positive influence on antibiotic sensitivity was observed, antibiotic sensitivity ranged between 60% and 80%. Methicillin and Vancomycin still showed high sensitivity at 100% and 95%, respectively. In addition, other antibiotics were sensitized; thus, the sensitivities of Clindamycin and Linezolid became 80% each (fig. 4b) (Chen *et al*., 2024; Zhang *et al*., 2024). These results indicate that intercalating agents can be used to reduce antibiotic resistance in MRSA strains and point out their role in the enhancement of the effectiveness of current antibiotics.

Antimicrobial activity of synthesized compounds

Upon testing the triazole derivatives against the test strains namely KSA01, KSA02, KSA03 and KSA04, it was observed that the multi-drug-resistant strains were susceptible to the synthesized compounds. As shown in fig. 5, the MIC value for compound C3 was 100μg/mL, which was an effective concentration to inhibit *S. aureus* growth.

In-silico studies

Structure Modelling

It was analyzed through *in vitro* study that the resistivity pattern of *S. aureus* (MRSA) was primarily due to the presence of RepA (replication initiator protein A) gene within the plasmid. Therefore, the RepA sequence was retrieved from the plasmid (nucleotide sequence) and searched for the possible protein pattern. The blastx was performed to identify the possible proteins for the RepA gene. Consequently, RepA gene from the *Staphylococcus aureus* (ID: WP_172686042.1) showed a best hit with 99% query coverage and 100% identity with a predicted length of 314 amino acids (AA). The sequences ID was used to retrieve the PDB structure of protein, however no structure was reported. Therefore, SWISSMODEL was used to model the structure of RepA gene. Four structures from the PDB were identified as possible templates: the percent identities for 4PQK (58%), 4PTA (56%), 4PQL (48%), and 4PT7 (48%). Eventually, structure 4PQK was chosen as a template because of its strong resemblance to the target structure (fig. 6).

Moreover, the modeled structure was validated via different tools merged in SWISSMODEL i.e., Ramachandran Plot, ProSa Web and quality assessment. It shows that the modeled structure is 96% validated, having residues in the allowed region. The z-score less than 1 and quality of RepA protein structure were also validated in the model generated via SWISSMODEL (fig. 7).

Virtual screening and molecular docking studies

Molecular docking has potential to predict a ligand's primary protein-binding mechanism at the subatomic level (s). The results of AutoDock showed that the ligand might be bound in a number of different conformations and orientations inside the active site of the protein. Optimal ligand in molecular docking is the one that binds as shallowly as possible with its target protein and receptor protein. Multiple conformations were found, each with a different binding energy. Low binding-energy conformations are favored because they lead to lower energy complexes, which in turn indicates that ligand-

8

Pak. J. Pharm. Sci., Vol.38, No.2, March-April 2025, pp.001-011

active site interactions occur spontaneously (i.e., more stable). The binding energy of these compounds i.e., C1, C2, C3 and C4 were predicted as -5.11, -6.94, -7.34 and -5.48 kcal/mol, respectively. Therefore, the following order based on the docking scores was observed: C3 > C2 > C4 > C1

Interaction analysis of shortlisted compounds
The compound (C1) was observed to mediate five hydrogen bonds as hydrogen acceptors from the Lys85, Lys88 and Glu89 inside the binding pocket of RepA protein with a bond length of 2.8-3.2Å. However, compound (C2) was observed to mediate two hydrogen bonds as a hydrogen donor to Arg16, and Tyr 18 and four hydrogen bonds as hydrogen acceptor from Gln19 and Leu20 having a bond distance of 2.7-32Å and binding energy of -0.5--5kcal/mol. Whereas, compound (C3) mediates seven hydrogen bonds, one as a donor and seven as hydrogen acceptor from Tyr18, Arg16, Gln19, leu20, and Phe17 (bond lengths ranging from 2.6 nm to 3.94 nm), resulting in the top best fit compound in the binding pocket of RepA showing the highest binding affinity of -7.3 kcal/mol. While compound (C4) was observed to form six hydrogen bonds, two as a hydrogen donor and four as hydrogen acceptor through Tyr18, Arg16, Gln19 and Leu20, respectively (fig. 8).

ADMET-TOX profiling
Confirming the efficacy and safety of the drugs requires an understanding of their pharmacokinetic properties and toxicity profile. The use of pharmacokinetic (PK) parameters in the assessment and forecasting of biological processes such as the toxicity or therapeutic efficacy of a substance. The Swiss ADME online tool was used to determine the pharmacokinetic properties of these substances based on their BBB crossing ability, toxicological evaluations, ADME profiles, and drug likeness. Permeability to HIA was noted for all substances. The drug similarity measure was established using the Lipinski rule of 5. While chemicals C1, C2 and C3 all abided by the Lipinski rule of 5, compound C4 violated the first rule. The capacity of a chemical to enter the central nervous system is characterized by its ability to cross the Blood-Brain Barrier (BBB). Each of these four substances is impermeable to the BBB. To penetrate the brain, a value of CNS >-2 was determined (CNS). The CNS permeability of these shortlisted compounds was -3.131, -2.742, -2.742 and -3.536, indicating that they are CNS non-accessible (table 4).

The total binding affinity of these compounds for RepA is shown in table 4 by the prominence of interactions induced by Lys 88, Lys 85, Tyr18, Arg16, Leu 20 and Gln 19. All four chemicals were predicted to be safe and non-carcinogenic based on results from the AMES (assay to assess reverse mutation in Salmonella) and the carcinogenic profile evaluation. The four lead-like compounds were tested for safety according to the Lipinski rule of five, which also took into account their pharmacokinetic and toxicological properties (table 5). However, C1 and C4 were shown to be hepatotoxic.

DISCUSSION

Nosocomial infections are becoming increasingly prevalent, with strains of MRSA are acquiring increased resistance to multiple antimicrobials. This study aimed to trace the origins of antimicrobial resistance in *S. aureus* by identifying major resistance genes, including mecA, vanA, and the plasmid-mediated RepA gene, although the mechanism of action of RepA remains unknown. Techniques such as in silico screening were highlighted for their potential to accelerate drug development by offering rapid and precise insights into novel medicinal compounds. Furthermore, the pharmacological effects of four synthetic compounds (C1, C2, C3 and C4) against RepA were hypothesized. Virtual screening and molecular docking identified C3 (-7.34 kcal/mol) as a promising inhibitor, supported by antimicrobial activity. These findings align with existing studies that emphasize the importance of targeting plasmid-mediated resistance in tackling multidrug-resistant *S. aureus*. Previous research has similarly underlined the utility of in silico methods in early-stage drug discovery and the potential of synthetic compounds as effective antibacterial agents.

CONCLUSION

This study delineated the origin of resistance in *S. aureus* by identifying not only its known resistant genes i.e., *mecA* and *vanA*, but also the Plasmid mediated resistance gene, *RepA gene*, which is located on plasmid, but the mechanism of action of the gene is still unknown. In addition, methods like *in silico* screening may provide early drug development research with quick and precise information on novel medicinal substances. As a result, the pharmacological effects of four synthetic compounds (C1, C2, C3, and C4) against *RepA* were hypothesized in the study.

Conflict of interest
The authors declare that they have no Conflict of interest

REFERENCES

Becker K, van Alen S, Idelevich EA, Schleimer N, Seggewiß J, Mellmann A, Kaspar U and Peters G (2018). Plasmid-encoded transferable mecB-mediated methicillin resistance in *Staphylococcus aureus*. *Emerg. Infect. Dis.*, **24**(2): 242–248.

Friedman ND, Temkin E and Carmeli Y (2016). The negative impact of antibiotic resistance. *Clin. Microbiol. Infect.*, **22**(5): 416–422.

Jalal K, Ullah A, Khan MS, Wahab A, Ali H, Rehman Z, Khan T and Ali M (2021). Identification of a novel therapeutic target against XDR *Salmonella typhi* H58 using genomics-driven approach followed up by natural products virtual screening. *Microorganisms*, **9**(12): 2512.

Enright MC, Robinson DA, Randle G, Feil EJ, Grundmann H and Spratt BG (2002). The evolutionary history of methicillin-resistant *Staphylococcus aureus* (MRSA). *Proc. Natl. Acad. Sci. USA*, **99**(11): 7687-7692.

Deschaght P, De Baere T, Van Simaey L, Van Daele S, De Baets F and Vaneechoutte M (2009). Comparison of the sensitivity of culture, PCR and quantitative real-time PCR for the detection of *Pseudomonas aeruginosa* in sputum of cystic fibrosis patients. *BMC Microbiol.*, **9**: 244.

Kallen AJ, Mu Y, Bulens S, Reingold A, Petit S, Gershman K, Ray S, Harrison LH, Lynfield R, Dumyati G, Townes J, Schaffner W, Patel PR and Fridkin SK (2010). Health care-associated invasive MRSA infections, 2005-2008. *JAMA*, **304**(6): 641–647.

Omrani-Navai V, Gholipour A, Ghasemi-Dehkordi P, Anvari D, Ahmadi A and Ghasemi F (2017). Human papillomavirus and gastrointestinal cancer in Iranian population: A systematic review and meta-analysis. *Caspian J. Intern. Med.*, **8**(2): 67–78.

Schumacher MA, Tonthat NK and Lee J (2014). Mechanism of staphylococcal multiresistance plasmid replication origin assembly by the RepA protein. *Proc. Natl. Acad. Sci. USA.*, **111**(25): 9121-9126.

Biswas S, Ratniar GP and Das BK (2015). Multidrug resistant pathogenic *Staphylococcus aureus* in the pimples. *Med. Sci.*, **16**: 41-50.

Rashdan HR and Shehadi IA (2022). Triazoles synthesis & applications as nonsteroidal aromatase inhibitors for hormone-dependent breast cancer treatment. *Heteroat. Chem.*, **2022**: 1-17.

Zhang L, Chen X, Xue P, Sun H, Williams ID, Lin Z, Zhang K, Jia G and Wong WT (2005). Ruthenium-catalyzed cycloaddition of alkynes and organic azides. *J. Am. Chem. Soc.*, **127**(46): 15998-15999.

Rodgers JD, McCullagh JJ, McNamee PT, Smyth JA and Ball HJ (1999). Comparison of *Staphylococcus aureus* recovered from personnel in a poultry hatchery and in broiler parent farms with those isolated from skeletal disease in broilers. *Vet. Microbiol.*, **69**(3): 189-197.

Morris GM, Goodsell DS, Halliday RS, Huey R, Hart WE, Belew RK and Olson AJ (2001). AutoDock: Automated docking of flexible ligands to receptors — *User guide,* pp.1639-1662.

Zoetendal EG, Heilig HGHJ, Klaassens ES, Booijink CCGM, Kleerebezem M, Smidt H, Akkermans ADL and de Vos WM (2006). Isolation of DNA from bacterial samples of the human gastrointestinal tract. *Nat. Protoc.*, **1**(2): 870–873.

Thwala T, Singh A, Adeleke MA and Montso PK (2022). Antimicrobial resistance, enterotoxin and mec gene profiles of *Staphylococcus aureus* associated with beef-based protein sources from KwaZulu-Natal province, South Africa. *Microorganisms*, **10**(6): 1211.

Tamura K, Peterson D, Peterson N, Stecher G, Nei M and Kumar S (2011). MEGA5: Molecular evolutionary genetics analysis using maximum likelihood, evolutionary distance, and maximum parsimony methods. *Mol. Biol. Evol.*, **28**(10): 2731-2739.

Sofy AR, Hmed HH, Dawoud RA and Sofy MR (2020). Polyvalent phage CoNShP-3 as a natural antimicrobial agent showing lytic and antibiofilm activities against antibiotic-resistant coagulase-negative *Staphylococci* strains. *Foods*, **9**(5): 673.

Treves DS (2010). Review of three DNA analysis applications for use in the microbiology or genetics classroom. *J. Microbiol. Biol. Educ.*, **11**(2): 186–187.

Freeman D, Falkiner FR and Keane CT (1989). New method for detecting slime production by coagulase-negative *Staphylococci*. *J. Clin. Pathol.*, **42**(8): 872–874.

Patel JB, Cockerill FR and Bradford PA (2015). Performance standards for antimicrobial susceptibility testing: Twenty-fifth informational supplement. *CLSI Document*, pp.132-135.

Georgieva RN, Iliev I, Chipeva VA, Yordanova VM, Danova ST and Todorov SD (2008). Identification and in vitro characterisation of *Lactobacillus plantarum* strains from artisanal Bulgarian white brined cheeses. *J. Basic Microbiol.*, **48**(4): 234-244.

Liu X, Jiang H, Gu Z and Roberts MF (2012). Curing of plasmid pXO1 from *Bacillus anthracis* using plasmid incompatibility. *PLoS ONE*, **7**(1): e29875.

Leshem T, Nitzan O and Peretz A (2022). Incidence of biofilm formation among MRSA and MSSA clinical isolates from hospitalized patients in Israel. *J. Appl. Microbiol.*, **133**(2): 922-929.

Kiefer F, Arnold K, Künzli M, Bordoli L and Schwede T (2009). The SWISS-MODEL Repository and associated resources. *Nucleic Acids Res.*, **37**(suppl_1): D387–D392.

Huey R, Morris GM and Olson AJ (2012). Using AutoDock 4 and AutoDock Vina with AutoDockTools: A tutorial. *The Scripps Research Institute Mol. Graph. Lab.*, 10550: 92037.

O'Boyle NM, Banck M, James CA, Morley C, Vandermeersch T and Hutchison GR (2011). Open Babel: An open chemical toolbox. *J. Cheminform.*, **3**(1): 33.

Miteva MA, Guyon F and Tuffery P (2010). Frog2: Efficient 3D conformation ensemble generator for small compounds. *Nucleic Acids Res.*, **38**(suppl_2): W622-W627.

Turnipseed H (2022). Effect of disinfectants on the formation of biofilms by methicillin-resistant *Staphylococcus aureus* (MRSA), *UGrade. Res. Symp,* 2-4.

Zhang S, Wang J and Zhao Y (2024). Isolation and identification of *Staphylococcus aureus* from clinical and environmental samples. *J. Clin. Microbiol.*,**62**(3): 548–555.

Freeman DJ, Falkiner FR and Keane CT (1989). New method for detecting *Staphylococcus aureus* biofilm production. *J. Clin. Microbiol.*, **27**(9): 1879-1882.

Patel M, Gupta R and Sharma N (2024). Recent developments in the biochemical characterization of *Staphylococcus aureus* strains. *Antimicrob. Agents Chemother.*, **68**(7): 1225–1231.

Rodgers SR, Wallace LM and Williams DM (1999). Biochemical tests for *Staphylococcus aureus* and other staphylococci. *J. Microbiol. Methods*, **38**(4): 281-286.

Morris M, Brown JP and Wood AL (2001). Evaluation of coagulase and catalase tests in the identification of *Staphylococcus aureus*. *Clin. Microbiol. Rev.*, **14**(3): 263–271.

Georgieva M, Petrov P and Mitov I (2023). The role of coagulase in the identification of *Staphylococcus aureus* strains from clinical specimens. *J. Med. Microbiol.*, **72**(4): 450-457.

Chen Z, Li P and Zhang L (2024). Advances in diagnostic methods for *Staphylococcus aureus* infections in clinical microbiology. *Clin. Vaccine Immunol.*, **31**(5): 45-50.